RECONSTRUCTION OF THE FRESNEL-CODED GAMMA CAMERA IMAGES BY DIGITAL COMPUTER

T. F. Budinger and B. Macdonald

Donner Laboratory and Lawrence Berkeley Laboratory, University of California, Berkeley, California

An algorithm for the digital reconstruction of the Fresnel-coded gamma camera image consists of the spatial Fourier transform of the hologram after applying a quadratic phase shift. Background subtraction is implemented by use of positive and negative zone plates. Tomographic planes are reconstructed in 27 sec from a single zone-plate shadow image by successively varying a parameter in the reconstruction algorithm on a small computer system.

This paper presents an algorithm for the digital reconstruction of the Fresnel zone-plate coded image and also experimental results with the gamma camera showing the tomographic potential of coded aperture imaging, the signal-to-noise ratio (SNR) comparison between zone-plate imaging and pinhole imaging, and the use of positive and negative zone plates for background subtraction.

The transmission efficiency is in the range of only 0.05% or less for a conventional parallel-hole or pinhole collimator. New techniques of coding such as multiple random pinhole-coded aperture imaging (*1–4*) and Fresnel zone-plate coding (*5–10*) have been suggested for gamma source imaging because the geometric efficiency of these schemes is 1,000 times or more greater than that of collimators in use today. In nuclear medicine studies, however, the sources are relatively large and therefore the effective efficiency of coded apertures is considerably less than their geometric efficiency. Consider an aperture (collimator) with N pinholes. The SNR will be improved by $\sqrt{N}$ times that of a single pinhole only if the image corresponding to each hole is separated from images of all other holes. A basic problem of coded aperture imaging in nuclear medicine is the fact that inherent noise increases as the side lobes of the spread function from one point source superimpose on the spread function of another point source. The advantage of increased collimator transmission for signal is lessened by the increase in inherent noise because of this spread function overlap. This fact has been recognized by Barrett and De Meester (*11*), who show that the SNR is reduced by a factor of $M^{-1/2}$ where M is the number of resolution elements because all photons from each resolution element contribute to the noise but only those photons originating from one resolution element contribute to the signal. In the limit of a very large souree this leads to a small disadvantage in exposure time required for the zone plate over the pinhole. Even an improvement in SNR by digital computer reconstruction cannot give results in less exposure time than the pinhole camera for extended objects. Moreover, Levy (*12*) argues that the gain in SNR of the Fresnel zone plate over that of the pinhole is proportional to the ratio of the intensity of the signal at each point to the average intensity in the whole image. There is real doubt, therefore, that the efficiency of the basic pinhole camera could be improved upon by Fresnel coding or other multi-aperture systems for simple two-dimensional imaging. Although there is no exposure time advantage of the Fresnel zone plate over the exposure time for a single pinhole aperture for extended objects, there is an inherent tomographic potential of the Fresnel-coded image (*13*) as well as the multiple random pinhole-coded image (*14*). To realize this potential for the Fresnel-coded image and to simplify reconstruction of the hologram without photographic transfer and optical bench manipulation, we developed a digital computer algorithm that will allow rapid reconstruction with most of the available new series of nuclear medicine computer systems interfaced to a gamma camera (*15*).

THEORY

Fresnel zone-plate imaging is done in two parts. First, the zone plate is used between the object and

Received Dec. 19, 1973; revision accepted Nov. 18, 1974.

For reprints contact: Thomas F. Budinger, Lawrence Berkeley Laboratory, Berkeley, Calif. 94720.

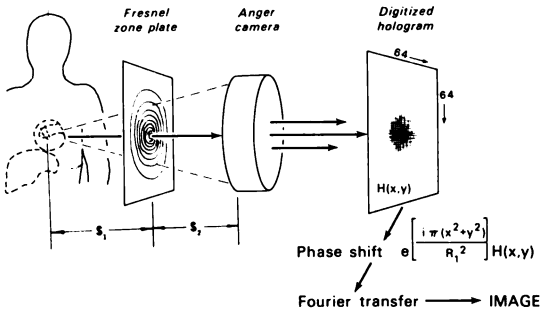

FIG. 1. Scheme of digital reconstruction of image from gamma camera.

detector to form a coded shadow $H(x_1,y_1)$ of the object on the detector (Fig. 1). This shadowgram is then placed in a coherent beam of light of wavelength λ, and an image $I(x,y)$ of the object is formed on a screen using the diffraction and focusing properties of the individual zone-plate shadows that make up the shadowgram. The image produced, according to the Huygens-Fresnel diffraction principle, is

$$I(x,y) = \iint H(x_1,y_1)\, A(x,y;x_1,y_1)\, dx_1 dy_1 \quad (1)$$

where

$$A(x,y;x_1,y_1) = \frac{1}{i\lambda f} \exp\left(\frac{i2\pi \ell}{\lambda}\right) \quad (2)$$

f being the distance between the shadowgram plane and the image plane and ℓ the path length traversed by a light ray between points in these two planes.

$$\ell = (f^2 + (x - x_1)^2 + (y - y_1)^2)^{1/2} = f\left(1 + \frac{(x - x_1)^2}{f} + \frac{(y - y_1)^2}{f}\right)^{1/2} \quad (3)$$

Assume that the square root term in Eq. 3 is adequately approximated by the first two terms in its binomial expansion. This is the Fresnel approximation and in effect is a replacement of the spherical Huygens' wavelet by quadratic surfaces (*16,17*). If we drop the constant phase term $\exp(i2\pi f/\lambda)/i\lambda f$, Eq. 2 becomes

$$A(x,y;x_1,y_1) = \exp\left(\frac{i2\pi}{2\lambda f}\{(x - x_1)^2 + (y - y_1)^2\}\right) \quad (4)$$

and Eq. 1 becomes

$$I(x,y) = \iint_{x_1 y_1} H(x_1,y_1) \exp\left(\frac{i\pi\{(x - x_1)^2 + (y - y_1)^2\}}{\lambda f}\right) dx_1 dy_1 \quad (5)$$

By regrouping terms after expanding the exponential, we have

$$I(x,y) = \exp\left(\frac{i\pi(x^2 + y^2)}{\lambda f}\right) \iint_{x_1 y_1} H(x_1,y_1) \exp\left(\frac{-i\pi(x_1^2 + y_1^2)}{\lambda f}\right) \exp\left(\frac{-i2\pi(xx_1 + yy_1)}{f\lambda}\right) dx_1 dy_1 \quad (6)$$

Note the operations of Eq. 6 involve merely the Fourier transform of the shadowgram times a phase shift function that is quadratic in the distance in the shadowgram plane from the optic axis.

It is well known that a Fresnel zone plate acts as a lens, and thus the image $I(x,y)$ is in focus when the distance f in Eq. 6 is chosen as the focal length of the shadow zone plate

$$f = \pm \frac{R_1^2}{\lambda} \quad (7)$$

where R_1 is the radius of the shadow of the first zone and λ is the wavelength. The radius of the first zone's shadow depends on the distance s_1 between the object plane and the zone plate and the distance s_2 between the zone plate and the camera (Fig. 1).

$$R_1 = R_0\left(1 + \frac{s_2}{s_1}\right) \quad (8)$$

where R_0 is the true radius of the zone plate. Substitution of Eq. 8 for the term λf in Eq. 6 gives the final algorithm:

$$I(x,y)^* = \mathcal{F}_2\left[H(x_1,y_1) \exp\left(\frac{i\pi(x_1^2 + y_1^2)}{R_1^2}\right)\right] \quad (9)$$

where $\mathcal{F}_2$ denotes a two-dimensional spatial Fourier transform that is easily implemented with a computer using the fast Fourier transform (FFT).

For the process described here with the on-axis zone plate, the virtual image, due to the dual sign in Eq. 7, is also present and superimposed on the true image. More important is a large DC component caused by object intensity and the zone-plate transmission both being non-negative. This background can be effectively eliminated by a method that does not involve the use of an off-axis zone plate with its attendant loss of resolution. The technique consists of subtracting the shadowgram obtained using a negative zone plate from that obtained using a positive zone plate (Fig. 2) (*18*). A similar procedure is applicable for random pinhole encoding (*19*). The basis for the method can be seen from an examination of the equations that govern image formation with the zone-plate system. The shadowgram H in Eq. 1 is just the convolution of the object intensity 0 with the transmission of the zone plate, either 1 + Z for a positive zone plate or 1 — Z for a negative zone plate. Thus, a positive zone plate shadowgram is

* I(x,y) is a complex amplitude. The image recorded is the modulus squared.

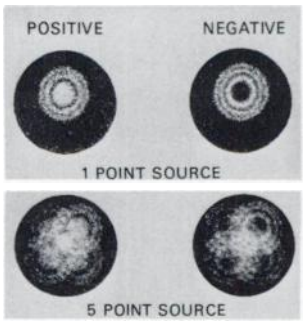

FIG. 2. Positive and negative Fresnel zone plates.

$$H_+ = 0 * (1 + Z) \quad (10)$$

where * denotes the convolution operation. The image, from Eq. 1 is

$$I_+ = H_+ * A = 0 * 1 * A + 0 * Z * A \quad (11)$$

The term 0 * 1 * A represents the large component of background. If one takes an exposure with a positive zone plate and obtains the shadowgram matrix $H_+ = 0 * (1 + Z)$ and a subsequent exposure with a negative zone plate, $H_- = 0 * (1 - Z)$, then the shadowgram matrix, which is the difference of these two matrices, yields an image that has no background.

$$I = (H_+ - H_-) * A = 0 * 2Z * A \quad (12)$$

The tomographic potential of the Fresnel-coded zone-plate aperture is implemented by performing a series of reconstructions varying the parameter R_1 corresponding to various focal planes given by Eq. 8. A given reconstruction plane s_1 is related to R_1 as

$$s_1 = \frac{R_0 s_2}{R_1 - R_0} \quad (13)$$

The zone-plate plane and camera plane are established perpendicular to and centered on the "optical" axis (Fig. 1). We used positive and negative zone plates with the center zone of 2.5-cm diam and only three rings in order to match the resolution of the gamma camera (Fig. 2). The camera events from ^{99m}Tc point sources were digitized in a 64 × 64 array using the Hewlett-Packard scintigraphic system 5407. The gains of the system were set to give 0.4 cm per picture element. Ten tomographic planes were established by varying R_1 of Eq. 9 in accordance with Eq. 8. For the results of Figs. 2 and 3, the distance from the zone plate to camera was 60 cm and the distance between the zone plate and object planes was varied between 15 and 25 cm in 1-cm increments.

After the digital phase shift is performed, the complex array is Fourier-transformed using a FFT algorithm which requires about 25 sec for a 64 × 64 complex array. The result for each plane is stored as an image frame and returned for viewing on a CRT from a disk file of image frames. The total operation takes 27 sec for each plane.

Positive-negative zone-plate subtraction technique for background elimination was accomplished by acquiring two shadowgrams, one with the positive zone plate and the other using the negative zone plate. Both were accurately centered. Distance from the zone plate to the camera was 73 cm and from zone plate to the sources was 62 cm. The result was obtained by subtracting the two shadowgrams and using the difference shadowgram to reconstruct the image. For comparison, a 3-mm pinhole collimator was used with the distance between the pinhole aperture and camera of 16 cm and the distance between aperture and sources of 13 cm.

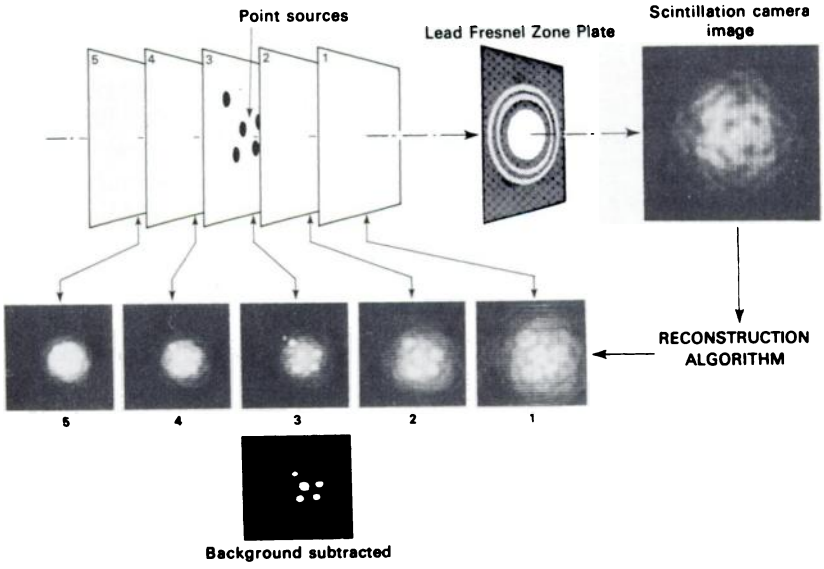

FIG. 3. Reconstruction of five sources of ^{99m}Tc separated by 1.5 cm in plane 90 cm from camera, 30 cm from zone-plate (first zone R_0 = 1.25 cm).

FIG. 4. Images from positive (A) and negative (B) zone plate reconstruction and results of image subtraction (C).

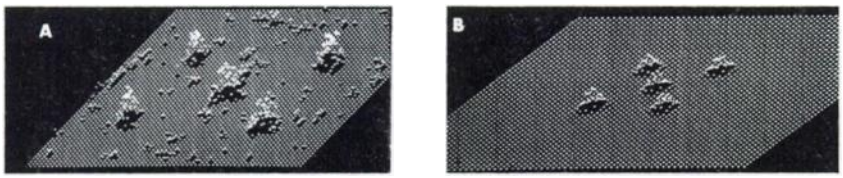

FIG. 5. Statistical comparison between zone-plate (A) and 3-mm aperture pinhole (B) images for identical data collection times (30 sec) with five point sources; distance from center is 3 cm.

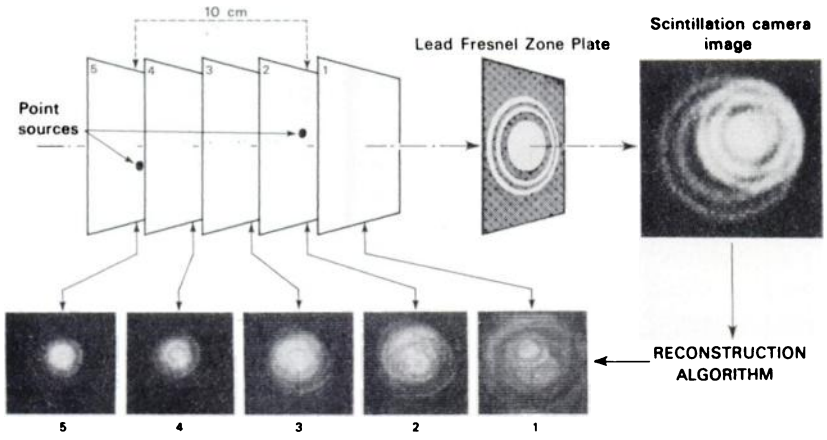

FIG. 6. Tomographic images of two point sources.

RESULTS AND DISCUSSION

The reconstruction of five small (2 mm) sources of ^{99m}Tc separated by about 2.0 cm is shown in Fig. 3. Background subtraction shown below the center image was performed by thresholding all intensities less than one-fourth the maximum intensity. A better method of background subtraction is to use the positive and negative zone-plate system (Fig. 4). A comparison of the positive/negative zone-plate image with the image using a pinhole collimator is given in Fig. 5. Using the zone plates 49,000 counts were detected from the five sources in 25 sec and the calculated (*11*) SNR was 40:1 with an expected lateral resolution of 5.5 mm FWHM. For the pinhole, 4,890 counts were collected from the five sources in 30 sec and the expected SNR is 31:1 with a lateral resolution of 5 mm.

This objective means of background subtraction makes easier a comparison between zone-plate and pinhole imaging. A complete analysis of the efficiency of a zone plate relative to a pinhole must take into account the effective field of view as well as the relative exposure times, the SNR, and the lateral resolution. With the same detector and geometry, the zone-plate field of view is much smaller than that for the single pinhole. The field of view can be increased by the use of a large multiwire chamber (*18*) in which case the lowered intrinsic efficiency of the gas proportional camera and the SNR for the Fresnel technique over the simple pinhole must be considered in assessing the relative efficiencies.

Quite apart from the efficiency question, Fresnel or other coded aperture systems have a potential value for tomography in nuclear medicine. The tomographic ability of this system is demonstrated in Fig. 6 where the Fresnel hologram of two point sources was processed. The blurring of the sources on planes adjacent to the focal plane can be quantitatively evaluated to give a measure of the tomographic capability of a particular zone-plate camera system.

ACKNOWLEDGMENTS

This work was performed under the support of the United States Atomic Energy Commission, with the assistance of William Hogan and John Harpootlian. We appreciate the interest and encouraging comments of Robert M. Glaeser and George W. Stroke.

REFERENCES

1. DICKE RH: Scatter hole cameras for x-rays and gamma rays. *Astrophys J* 153: L101–L106, 1968

2. HAYAT GS: *X-ray and Gamma Ray Imaging with Multiple Pinhole Cameras*, Ph.D. thesis, State University of New York at Stony Brook, 1971

3. GROH G, HAYAT GS, STROKE GW: X-ray and gamma ray imaging with multiple pinhole cameras using *a posteriori* image synthesis. *Appl Opt* 11: 191–193, 1972

4. WOUTERS A, SIMON KM, HIRSCHBERG JG: Direct method of decoding multiple images. *Appl Opt* 12: 1871–1873, 1973

5. BARRETT HH: Fresnel zone plate imaging in nuclear medicine. *J Nucl Med* 13: 382–385, 1972

6. BARRETT HH, DE MEESTER GD, WILSON DT: Recent advances in Fresnel zone-plate imaging. In *Medical Radioisotope Scintigraphy 1972*, vol 1, Vienna, IAEA, 1973, pp 269–284

7. ROGERS WL, HAN KS, JONES LW, et al: Application of a Fresnel zone plate to gamma-ray imaging. *J Nucl Med* 13: 612–615, 1972

8. BARRETT HH, WILSON DT, DE MEESTER GD, et al: Fresnel zone plate imaging in radiology and nuclear medicine. *Opt Eng* 12: 8–12, 1973

9. ROGERS WL, JONES LW, BEIERWALTES WH: Imaging in nuclear medicine with incoherent holography. *Opt Eng* 12: 13–22, 1973

10. TIPTON MD, DOWDY JE, CAULFIELD JH: Coded aperture imaging with on-axis Fresnel zone plates. *Opt Eng* 12: 166–168, 1973

11. BARRETT HH, DE MEESTER GD: Quantum noise in Fresnel zone-plate imaging. *Appl Opt* 13: 1100–1109, 1974

12. LEVY G: Comment on "Fresnel zone plate imaging in nuclear medicine." *J Nucl Med* 15: 214–215, 1974

13. BARRETT HH, DE MEESTER GD, et al: Tomographic imaging with a Fresnel zone-plate system. In *Tomographic Imaging in Nuclear Medicine*, Freedman GS, ed, New York, Society of Nuclear Medicine, 1973, pp 106–121

14. CHANG L-T, KAPLAN S, MACDONALD B, et al: *A Method of Tomographic Imaging Using a Multiple Pinhole Coded Aperture*. University of California Lawrence Berkeley Laboratory Report 3001, 1974

15. BUDINGER TF: Clinical and research quantitative nuclear medicine system. In *Medical Radioisotope Scintigraphy 1972*, vol 1, Vienna, IAEA, 1973, pp 501–555

16. GOODMAN JA: *Introduction to Fourier Optics*, New York, McGraw-Hill, 1971, pp 57–60

17. BORN M, WOLF E: *Principles of Optics*, 2nd rev ed, Oxford, Pergamon Press, 1964

18. MACDONALD B, CHANG L-T, PEREZ-MENDEZ V, et al: Gamma-ray imaging using a Fresnel zone-plate aperture, multiwire proportional chamber detector, and computer reconstruction. *IEEE* NS 21: 678–684, 1974

19. BLAKE RL, BUREK AJ, FENIMORE E, et al: Solar x-ray photography with multiplex pinhole camera. *Rev Sci Instrum* 45: 513–516, 1974